

Magnetic Field Gradients in NMR: Friend or Foe?

Timothy J. Norwood

Department of Chemistry, Leicester University, University Road, Leicester, LE1 7RH, U.K.

1 Introduction

Anyone who has used an NMR spectrometer is familiar with magnetic field gradients. In the form of inhomogeneities in the static field of the magnet they cause broadening of the spectral lines, often hindering analysis. Although this somewhat negative manifestation of the phenomena is the first experience of most spectroscopists, a growing appreciation of their practical uses has resulted in some of the most important developments in NMR methodology over recent years, often extending its uses far beyond its traditional role as an analytical tool for chemists. The exploitation of the properties of magnetic field gradients is at the heart of magnetic resonance imaging (MRI); this technique is now widely used as an aid to clinical diagnosis in many hospitals and is proving to be a promising tool for addressing chemical problems. Magnetic field gradients are also fundamental to NMR techniques for studying diffusion, which have proved invaluable for studying the microscopic structure of heterogeneous systems. A further use for magnetic field gradients that has come to maturity over the past few years is in replacing phase cycling in many multiple-pulse experiments, enabling cleaner spectra to be obtained in shorter times.

In this article we examine the place of magnetic field gradients in pulsed Fourier transform NMR from two perspectives: as a problem and as a solution to problems.

2 Magnetic Field Inhomogeneity

NMR is concerned with the precession of nuclear magnetic moments in an applied magnetic field, B_0 . In a perfectly homogeneous magnetic field the precessional frequency of the nuclear spins, the Larmor frequency ω is given by:

$$\omega = \gamma(1 - \sigma)B_0, \quad (1)$$

where γ is the magnetogyric ratio and σ is the shielding constant which is responsible for chemical shift. In a conventional one-dimensional NMR spectrum nuclear spins in different chemical environments will each give rise to a peak at a characteristic frequency ω . If B_0 is not homogeneous, but exhibits spatially

dependent magnetic field inhomogeneity $\Delta B_0(\mathbf{r})$, then the effective Larmor frequency, ω_{eff} , will become

$$\omega_{\text{eff}} = \omega + \gamma(1 - \sigma)\Delta B_0(\mathbf{r}). \quad (2)$$

Since $\sigma \ll 1$, and as it is usually the case that $\Delta B_0(\mathbf{r}) \ll B_0$, equation 2 can be reduced to

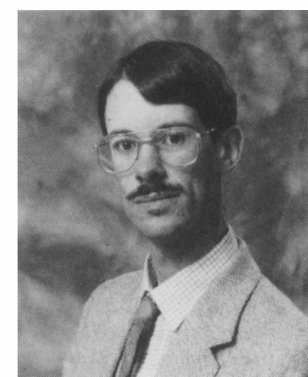
$$\omega_{\text{eff}} = \omega + \gamma\Delta B_0(\mathbf{r}). \quad (3)$$

It is clear from this equation that as the magnetic field varies across the sample so will the Larmor frequency of the nuclei.

At equilibrium, the nuclear magnetization of a sample gives rise to a static net-magnetization vector in the direction of B_0 (by convention, the z -axis). To observe a free induction decay the magnetization vector must first be rotated into the xy -plane; this is achieved by applying a pulse of coherent radiofrequency radiation. By adjusting the power, length, and phase of the pulse, it is possible to determine both the angle the pulse will rotate the nuclear magnetization through, and the axis in the xy -plane about which it will be rotated; for example a 90_x° pulse will rotate the magnetization through 90° about the x -axis. After the application of a 90_x° pulse to the equilibrium magnetization, the net-magnetization vector will be found along the y -axis. The subsequent evolution of this transverse magnetization vector in both homogeneous and inhomogeneous magnetic fields, the resulting free induction decays (fid) and Fourier transformed spectra are sketched in Figure 1. In a homogeneous magnetic field the magnetization vector precesses at a single frequency and gives rise to a free induction decay that decays solely due to transverse relaxation. In an inhomogeneous magnetic field the magnetization vector has to be subdivided into a number of smaller vectors, each precessing at a different frequency. These vectors spread out (dephase) as they evolve, resulting in a reduction in the size of the net transverse magnetization of the sample, causing the free induction decay to disappear more rapidly and the line in the NMR spectrum to broaden. In the extreme, the inhomogeneity-broadened lines of a spectrum may coalesce into a featureless hump. In some applications, magnetic field gradients are used to deliberately dephase the transverse magnetization.

Magnetic field variations across a sample can have two main origins: inhomogeneities in the applied magnetic field and variations in magnetic susceptibility across the sample. In a

Tim Norwood did his B.Sc. at King's College London (1983),



an M.Sc. at the University of British Columbia (1985), and his Ph.D. at Cambridge University with Professor Laurie Hall (1989). After two post-doctoral years with Dr. I. D. Campbell at Oxford University he took up his present position as a lecturer in physical chemistry at Leicester University. His research interests include the design and application of NMR spectroscopic and imaging techniques for addressing biological problems.

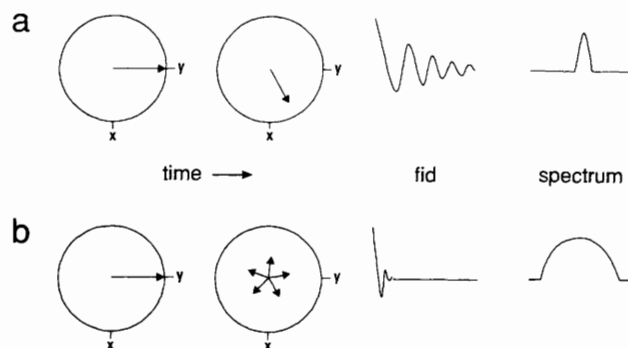


Figure 1 The evolution, resulting free induction decay (fid), and spectrum of a transverse magnetization vector in (a) a homogeneous and (b) an inhomogeneous magnetic field.

homogeneous liquid in an NMR tube magnetic susceptibility variations arise at the solution-glass-air and solution-air interfaces. Since NMR tubes have axial symmetry, the resulting variations in the magnetic field are also symmetric and can be counteracted by applying small additional magnetic field gradients across the sample using the spectrometer's shim coils. However, this compensation measure may fail if the sample is either particularly large or heterogeneous. Large samples are often encountered in *in vivo* imaging or spectroscopic studies of living systems, and those encountered in applications to geology and material science as well as biological systems are often extremely heterogeneous. The microscopic but often extremely strong magnetic field gradients generated in heterogeneous samples as a result of variations in magnetic susceptibility can obliterate any features in the spectrum and are impervious to shimming.

The problems presented by the presence of unwanted magnetic field gradients can be tackled in two ways: by using echo-based experiments designed to reverse their effects, and by using zero-quantum coherence which is unaffected by magnetic field gradients.

3 Counteracting the Effects of Magnetic Field Gradients: Echos

Some NMR measurements are more susceptible to the effects of unwanted magnetic field gradients than others. In a perfectly uniform magnetic field, the transverse relaxation time T_2 can be measured from the free induction decay or from peaks in the spectrum since the natural line width at half peak height is equal to $(1/\pi T_2)$. However, transverse relaxation time measurements are particularly vulnerable to variations in the magnetic field since even gradients that are not immediately obvious from the appearance of the spectrum can cause large errors in their apparent values. For example, gradients causing as little as 0.1 Hz line broadening will result in an error of 50% for a T_2 of 1.6 s or 20% for a T_2 of 0.64 s.

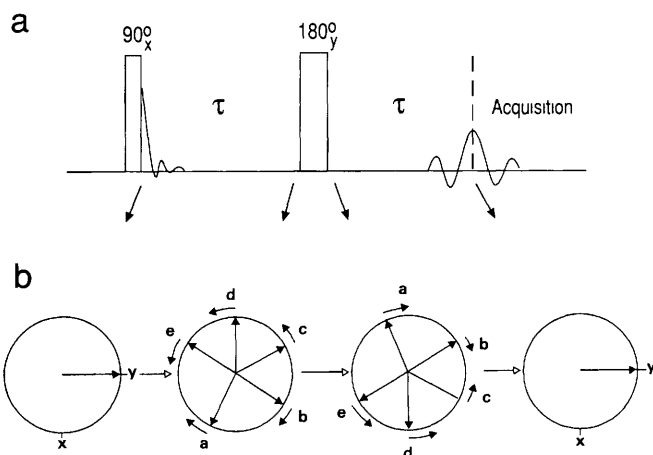


Figure 2 (a) Pulse sequence for the spin echo experiment (b) Vector model representation of the evolution of transverse magnetization during a spin echo

Transverse relaxation times can be measured independent of the effects of magnetic field gradients by using an experiment based on a spin echo.¹ Figure 2. This experiment is explained using the vector model in the figure. The transverse magnetization excited by the first pulse is subsequently allowed to evolve due to its chemical shift, scalar couplings (not included in this example), and magnetic field inhomogeneity during τ . In this example, the last factor has caused the transverse magnetization to dephase entirely at the end of this period. The 180° pulse, often known as a refocusing pulse, rotates all the nuclear magnetization vectors through 180° about the y -axis. This rearranges the positions of the dephased vectors such that while they would

previously have continued to spread out, subsequent evolution during the second τ period will cause them to come back together, reversing the evolution due to chemical shift and magnetic field gradients during the first τ period. Consequently, all that will have happened by the end of this sequence of events, when the free induction decay is acquired, is decay of the magnetization due to T_2 and evolution due to any scalar couplings present. The intensity of the observed signal will therefore be given by

$$I(2\tau) = I(0)\exp(-2\tau/T_2) \quad (4)$$

Consequently T_2 can be readily calculated from a series of measurements at different values of τ . Spin echos are incorporated into many NMR experiments to reverse the effects of magnetic field inhomogeneity.

A number of two-dimensional experiments based upon the use of echos produce F_1 spectra that are unaffected by magnetic field inhomogeneity.²⁻⁴ The 2D-J experiment,² which correlates the chemical shift of a spin in F_2 with its multiplet in F_1 , is perhaps the best known example. However, in all of these experiments, if the magnetic field gradients present are strong, signal may also be lost due to diffusion (see below). Besides distorting T_2 values, this effect may also broaden the lines of the F_1 spectra produced by these experiments. In the case of T_2 measurements, diffusion-attenuation can be overcome by replacing the single spin echo with a train of closely spaced 180° pulses⁵ differing in phase from the excitation pulse by 90°.

4 High Resolution Spectroscopy in the presence of Magnetic Field Gradients: Zero-Quantum Coherence

Many of the samples of interest in geological and material science applications of NMR are by nature heterogeneous, and consequently high resolution spectra cannot be obtained from them using conventional methods. In this context the possibilities opened up by exploiting the properties of zero-quantum coherence are particularly exciting since zero-quantum spectra are unaffected by magnetic field gradients.

The signal observed in the conventional NMR spectrum arises from single-quantum coherence. A single-quantum coherence is a phase coherence between two states for which $\Delta M = \pm 1$, where

$$\Delta M = \sum_k \Delta m_k, \quad (5)$$

and Δm_k is the change in magnetic quantum number of a spin k between the two states concerned. Those spins that have 'flipped' between the two states are said to be active in the coherence. Single-quantum coherence can be detected because it has a net magnetization vector associated with it, Figure 3A. An energy level diagram of a scalar coupled two-spin system is sketched in Figure 4. In addition to the four allowed single-quantum transitions it can be seen that there are two additional transition possibilities: a double-quantum transition for which $\Delta M = \pm 2$ and a zero-quantum transition for which $\Delta M = 0$. The coherences to which these transitions give rise are 'spin forbidden' since $\Delta M \neq \pm 1$ and consequently they cannot be excited by the application of a single non-selective pulse to the equilibrium magnetization of a spin system. Neither can they be observed since they have no net magnetization associated with them, Figure 3B. However, these *multiple-quantum coherences*⁶⁻⁸ can be studied indirectly, typically in a two-dimensional experiment, Figure 5, multiple-quantum coherence is excited indirectly using a sequence of pulses and delays and detected indirectly following its conversion into observable single-quantum coherence. In such experiments the extent of multiple-quantum evolution during the evolution period t_1 is reflected in the phase and amplitude of the observed single-quantum coherence. By repeating the experiment, whilst systematically incrementing t_1 , and then Fourier transforming the

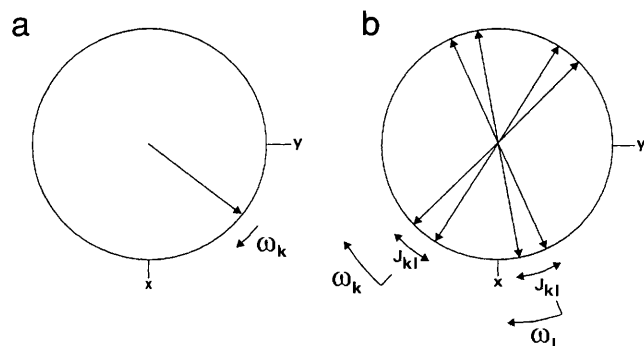
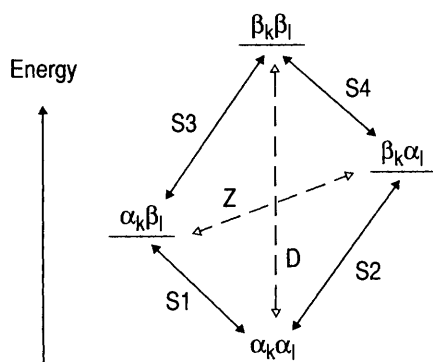


Figure 3 Vector model representations of (a) a single-quantum coherence of an uncoupled spin k and (b) a two-spin multiple-quantum coherence between a pair of coupled spins k and l , within the limitations of this model, it may correspond to either a zero- or double-quantum coherence

Energy level diagram



Spectrum

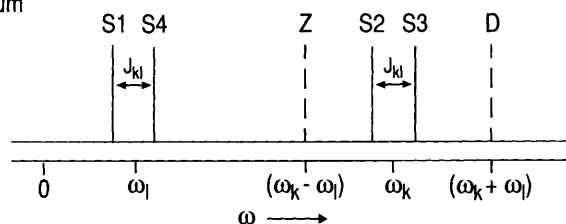


Figure 4 Energy level diagram and spectrum for a pair of coupled spins k and l . Allowed transitions and peaks are indicated by continuous lines while forbidden transitions and peaks are indicated by dashed lines. A transition is allowed when $\Delta M = \pm 1$ and is forbidden otherwise. α and β correspond to the two states ($m = +\frac{1}{2}$ and $-\frac{1}{2}$ respectively) of a spin- $\frac{1}{2}$ nucleus. Zero-, single-, and double-quantum transitions are denoted by Z , S , and D respectively

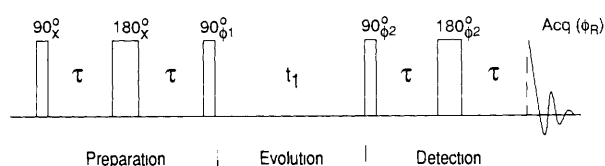


Figure 5 Pulse sequence for multiple-quantum spectroscopy. Since multiple-quantum coherence violates the rules for allowed transitions, it is excited and detected indirectly using a sequence of pulses and delays, multiple-quantum coherence evolves during the evolution period t_1 . A multiple-quantum spectrum can be obtained in a two-dimensional experiment by repeating the experiment while systematically incrementing t_1 and then Fourier transforming the data with respect to t_1 . Typically, $\tau = (\frac{1}{2} J)$. Even orders of coherence are excited when $\phi_1 = x$ and odd when $\phi_1 = y$. A given order of coherence can be selected by phase cycling ϕ_2 and ϕ_R . In the presence of a magnetic field gradient, only zero-quantum coherence will be observed since all other orders will be dephased during t_1 .

resulting data matrix with respect to t_1 , a multiple-quantum spectrum can be obtained. Multiple-quantum coherence is of interest here because of its sensitivity to magnetic field gradients. When modified to include multiple-quantum coherence equation 3 becomes

$$\omega_{\text{MQC}} = \sum_k \Delta m_k [\omega_k + \gamma k \Delta B_0(r)] \quad (6)$$

It can be seen from equation 6 that a coherence's sensitivity to magnetic field gradients will be proportional to its order. Thus, while homonuclear double-quantum coherence will be twice as sensitive as single-quantum coherence to a magnetic field gradient, zero-quantum coherence will be completely unaffected by it. Consequently, the zero-quantum spectrum will always be at high resolution, regardless of any magnetic field gradients present.⁹ Unlike echo-based techniques, zero-quantum spectra are unaffected by diffusion.

From equation 5 it can be seen that a minimum of two spins are required to excite a zero-quantum coherence. For the pulse sequence given in Figure 5 to be effective, a given pair of spins must either have a mutual scalar coupling or both must have scalar couplings to a common third spin for a coherence to be excited between them. Therefore a zero- or double-quantum coherence cannot be excited from water, for example. Multiple-quantum spectra do not have the appearance of conventional spectra. From equation 6 it can be seen that a two-spin zero-quantum coherence will have a frequency that is the difference in Larmor frequencies of its two active spins. This is illustrated for a two-spin system in Figure 4. Furthermore, scalar couplings, which will only be observed to spins l not active in the coherence (and not between those spins k active in it), will also correspond to linear combinations of those found in the conventional single-quantum spectrum.

$$J_{\text{MQC}} = \sum_k \Delta m_k J_{kl} \quad (7)$$

In the case of a two-spin system (Figure 4), since both spins must be active in either a zero- or double-quantum coherence, both spectra will only contain a singlet.

Consequently, the zero-quantum spectrum (and multiple-quantum spectra in general) will have an unfamiliar appearance and cannot be interpreted in the conventional manner. However, alternative methods for analysing zero-quantum spectra have been developed.⁸

An intriguing feature of multiple-quantum coherence is highlighted by the vector model representation given in Figure 3B. This picture can represent a zero-quantum coherence between two spins k and l which we know from equation 6 will precess at the frequency $(\omega_k - \omega_l)$. However, no vector in this picture actually evolves at this frequency, the antiphase k -spin vectors evolve at $\omega_k \pm J_{kl}/2$, and the antiphase l -spin vectors evolve at $\omega_l \pm J_{kl}/2$. The properties of a multiple-quantum coherence only become apparent when it is converted into single-quantum coherence for detection; the efficiency of this process depends upon the difference in phases of the k and l spin antiphase vectors and consequently on $(\omega_k - \omega_l)$ for a zero-quantum coherence.

The zero-quantum spectrum of an A(MK)X spin system – the four aromatic protons of salicylic acid – acquired in an inhomogeneous magnetic field with the pulse sequence sketched in Figure 5, is given in Figure 6c. The zero-quantum spectrum is clearly at high resolution even though the conventional spectrum acquired under the same conditions, Figure 6b, is little more than a broad featureless hump. The zero-quantum spectrum is symmetrical about the centre, the zero-frequency peak does not arise from zero-quantum coherence but is an artifact arising from magnetization that was longitudinal during the evolution period. There is a zero-quantum coherence between each pair of adjacent protons, which occurs at the difference of their Larmor frequencies in the conventional high resolution spectrum, Figure 6a.

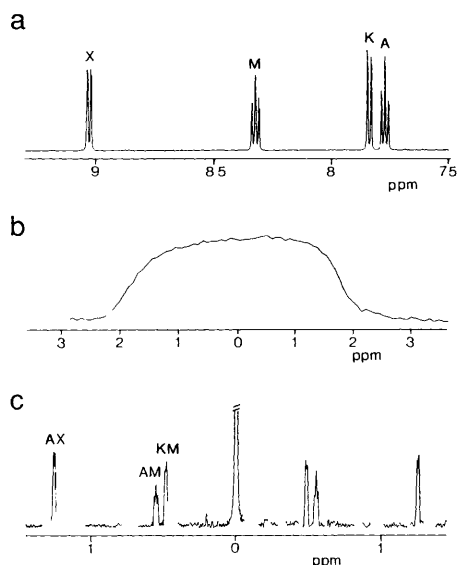


Figure 6 500 MHz ^1H spectra of the aromatic protons of salicylic acid (a) Conventional (single-quantum) spectrum acquired in a homogeneous magnetic field (b) Conventional spectrum acquired in the presence of a magnetic field gradient (c) Zero-quantum spectrum acquired in the presence of the same magnetic field gradient as (b)

5 Measurement of Diffusion

In the physical sciences, self-diffusion data have been shown to be a valuable source of information on molecular organization and phase structure, while, in the context of magnetic resonance imaging, diffusion-contrast has been found useful as an aid to the clinical diagnosis of a number of diseases

As has already been noted, diffusion through a magnetic field gradient can cause attenuation of the signal obtained in a spin echo experiment. Whilst this phenomenon is a problem in the context of T_2 measurement, it has been turned to good use in a series of NMR experiments designed to study diffusion. Traditionally, self-diffusion coefficients were measured using radioactive tracer techniques. Although extremely accurate, such studies take days, or even weeks, for a single component and require isotopic labelling. NMR techniques have proved to be an attractive alternative since they can provide accurate diffusion coefficients of multicomponent systems in a matter of minutes, and without the need for isotopic substitution. The most commonly used NMR experiment for measuring diffusion, the pulsed gradient spin echo (PGSE) method,^{10–11} is sketched in Figure 7a. It consists of a spin echo and a pair of magnetic field

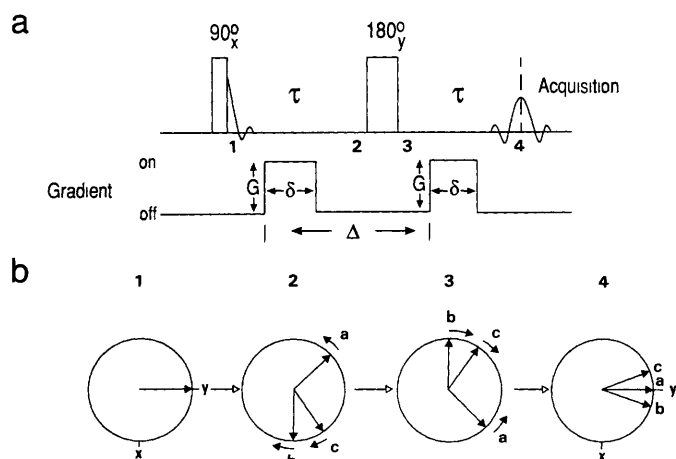


Figure 7 (a) Pulsed gradient spin echo (PGSE) pulse sequence for measuring diffusion (b) Vector model representation of the evolution of diffusing transverse magnetization during a PGSE experiment

gradient pulses, one either side of the 180° pulse. The static magnetic field B_0 is assumed to be homogeneous. How PGSE works can best be appreciated by considering one of the criteria for echo formation in the spin echo experiment. For evolution during the first half of the spin echo to be completely reversed by the end of the second half of the experiment, the frequencies of individual nuclei must remain constant throughout. However, if a magnetic field gradient is present, the frequency of the nuclei will vary with their position in the direction of the gradient. Consequently, any motion, such as that due to diffusion, in the direction of the gradient will result in a change in frequency. The effect of this on echo formation is illustrated in Figure 7b. Three vectors are considered: *a* does not move in the direction of the gradient during the experiment and so its frequency remains constant and it ends up along the *y*-axis; *b* moves in the direction of increasing magnetic field strength between the two halves of the experiment and consequently its frequency is greater during the second half, and as a result it 'overshoots' the *y*-axis; *c* moves in the direction of decreasing magnetic field strength between the two halves of the experiment resulting in a decrease in frequency as a consequence of which it 'undershoots' the *y*-axis. Clearly, diffusion will result in a dispersion of vectors about the *y*-axis instead of alignment along it, and consequently the overall intensity of the echo will be reduced. The intensity of the echo produced in the PGSE experiment is given by

$$I(2\tau) = I(0)\exp[-2\tau/T_2 - (\gamma G\delta)^2 D(\Delta - \delta/3)], \quad (8)$$

where G is the intensity of the magnetic field gradient, δ is the duration of each gradient pulse, Δ is the time between the start of the two gradient pulses, and D is the diffusion coefficient. It can be seen from equation 8 that a plot of $\log_e[I(2\tau)]$ against $\delta^2(\Delta - \delta/3)$ will have a gradient of $-(\gamma G)^2 D$ from which D can be calculated. Data are usually acquired for several values of G while keeping all other parameters constant.

In heterogeneous systems the diffusing molecules may encounter a barrier to their motion, for example particles in a suspension or cell walls in biological tissue. Under these circumstances, diffusion is said to be restricted. Restricted diffusion can be detected with the PGSE experiment.^{11–12} If diffusion is measured with a short echo time, the diffusing molecules will not have moved very far and therefore few will have experienced any restriction, consequently the apparent value of the diffusion coefficient will be close to the unrestricted value. As the echo time of the PGSE experiment is increased, so the fraction of molecules that experience restriction will also increase and will therefore have moved over small distances than they otherwise would have, consequently the apparent value of the diffusion coefficient will decrease. A typical plot showing the variation of the apparent value of the diffusion coefficient as a function of echo time is sketched in Figure 8. By modelling such data it is possible to determine values for the parameters associated with restriction. For example, from the diffusion of water in biological tissue, cell size and permeability can be determined.

Pulse sequences for measuring diffusion have been incorporated into a number of magnetic resonance imaging experiments to produce images in which the signal intensity reflects the diffusion coefficient. The environment of the diffusing molecules as well as their concentration can be mapped using such techniques.¹³ Diffusion coefficient maps can also be generated from such data. Diffusion-contrasted imaging *in vivo* has been shown to be useful in determining the regions of the brain affected by stroke and multiple sclerosis.

We have noted that the sensitivity of a coherence to magnetic field gradients is proportional to its order. Consequently, by using a higher order of coherence, the sensitivity of the PGSE experiment to diffusion can be increased, allowing diffusion coefficients to be determined more accurately or a lower gradient strength to be used.¹⁴ A multiple-quantum PGSE experiment can be constructed by placing PGSE, minus the first 90° pulse, into the evolution period of the multiple-quantum experiment sketched in Figure 5.

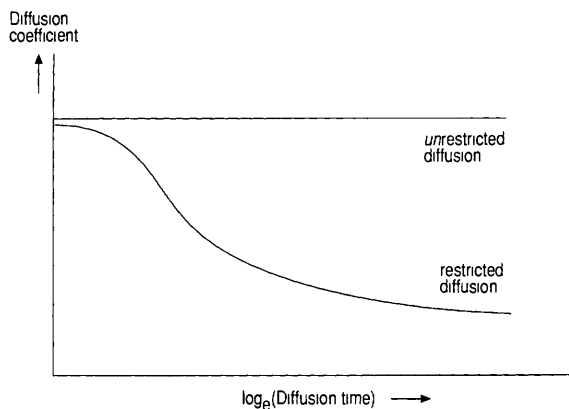


Figure 8 Variation of the apparent diffusion coefficient as a function of the diffusion time (t in Figure 7) for unrestricted and restricted diffusion

The use of pulsed magnetic field gradients in both this and other applications has one major problem associated with it. When a magnetic field gradient is switched on or off the change in magnetic flux induces electrical currents in nearby metal, i_e in the probe and magnet. These eddy currents can persist for seconds and have the effect of distorting the spectrum, sometimes beyond recognition. This problem can be overcome by using gradients which are shielded so that their effects are not felt outside their immediate volume,¹⁵ these are only now becoming widely available.

6 Imaging

In the two decades since its inception, imaging has become not only the most important application of magnetic field gradients in NMR, but one of the most important applications of NMR as a whole, familiar to most people as magnetic resonance imaging or MRI.¹⁶⁻¹⁷ The word 'nuclear' is omitted so as not to distress patients!

Although imaging can be implemented in many different ways, the earliest method remains the best for explaining the fundamental principles.¹⁶ Consider a sample consisting of two tubes of water, Figure 9. In a uniform magnetic field a single peak is observed in the NMR spectrum since all the molecules will precess at the same frequency, equation 1, regardless of their spatial location. If a linear magnetic field gradient is applied across the sample, in this example in the x -direction, then, analogously to equation 3, equation 1 will become

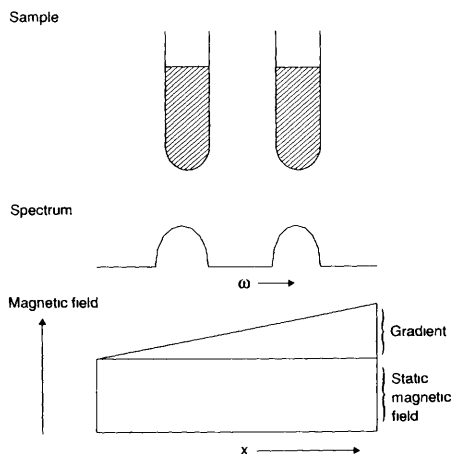


Figure 9 The principle of one-dimensional NMR imaging. The application of a magnetic field gradient across a sample will give rise to a frequency offset proportional to its spatial location in the direction of the gradient, thus making the spectrum a profile of the sample in the direction of the gradient.

$$\omega_{\text{eff}} = \omega + \gamma x G_x, \tag{9}$$

where G_x is the strength of the magnetic field gradient and x is the spatial coordinate. Clearly, the Larmor frequency of the water will now increase linearly across the sample as a function of its x -coordinate, and the spectrum, Figure 9, will become a one-dimensional image or profile of the sample.

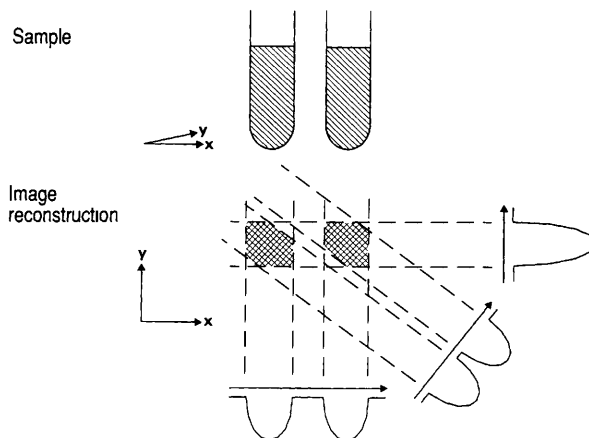


Figure 10 The principles of constructing a two-dimensional NMR image using back projection. A number of profiles of the sample are obtained with different orientations which are then used to construct a two-dimensional image. Profiles with different orientations are obtained by acquiring spectra in the presence of magnetic field gradients in different directions (indicated by arrows), an x -gradient will result in an x -profile while a y -gradient will result in a y -profile of the sample.

The principles of two-dimensional imaging are illustrated in Figure 10. Here, by using combinations of two gradients G_x and G_y , a series of one-dimensional images are obtained in different directions in the xy -plane. A two-dimensional image of the object can be reconstructed from these one-dimensional projections using a technique known as back projection reconstruction, as illustrated in the figure. Clearly, the greater the number of profiles used to construct an image, the better defined it will be. This method can be extended to three dimensions. At the present the most widely used imaging experiments are based on multi-dimensional Fourier transformation rather than back projection.¹⁶

The intensity of a given element of an NMR image can reflect a number of factors, depending on the structure of the pulse sequence used. In addition to the concentration of the observed species, the image intensity may also reflect its transverse or longitudinal relaxation times or its diffusion coefficient. It is possible to produce separate images of different chemical species. An NMR image of a guinea pig is given in Figure 11, here the contrast reflects the concentration of mobile protons and their transverse relaxation times.

Although, as a result of the quality of the anatomical detail it provides and its non-invasive nature, NMR imaging is most widely used as a clinical tool, a number of chemical applications have also been explored. Often the changes occurring within a system are observed indirectly. An example is given in Figure 12 where the spatial progression of a change in a chemical equilibrium through a gel is monitored.¹⁸ The chemical equilibrium, the chelation of aqueous copper by ethylenediaminetetraacetic acid, is pH-dependent. Initially the gel has a pH of 7. An acidic solution is added to the central well and diffuses out through the gel, causing a change in pH as it does so, and thus shifting the equilibrium towards free Cu^{2+} . The image intensity reflects the concentration of the water, which is the main observed species, and its transverse and longitudinal relaxation times. The free Cu^{2+} is particularly good at increasing the longitudinal relaxation rate of the water, which, with the pulse sequence used here, results in a region of low signal intensity. Since a single Cu^{2+} ion

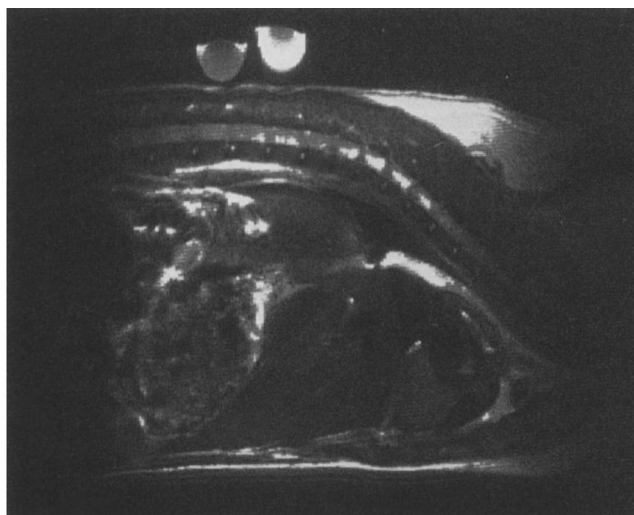


Figure 11 ^1H NMR image of the body of a live guinea pig under anaesthetic. The spinal column runs across the top of the image, while from right to left can be seen the heart, liver, and stomach. The oesophagus extends from above the heart to the stomach. Two reference tubes can be seen at the top of the image.

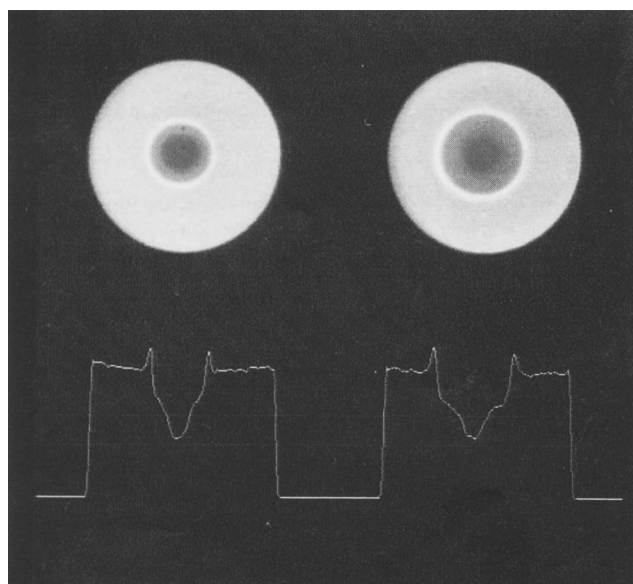


Figure 12 ^1H NMR images illustrating the shift in the equilibrium of the chelation of aqueous copper by ethylenediaminetetraacetic acid (EDTA) in a gel under the influence of a pH gradient (see text). The left and right images were acquired 4 and 25 minutes respectively after the addition of acid to the central well. Traces through the two images are given at the bottom of the figure.¹⁸

can help relax many water molecules, techniques of this type can enable changes to be observed in species that have too low a concentration to be observed directly.

7 Magnetic Field Gradient Pulses: An Alternative to Phase Cycling

A pulse sequence consists of a series of radiofrequency (r.f.) pulses and delays. Each pulse is assumed to rotate the nuclear magnetization through a specific angle about a specific axis. However, in practice, mis-setting of pulse angles, r.f. inhomogeneity across the sample, and resonance offset effects all give rise to non-ideal behaviour. As a result of this not all of the nuclear magnetization will evolve as expected during an experiment. For

example, although an ideal 180° pulse inverts all of the longitudinal magnetization of a sample, in practice, due to the effects noted above, some will end up as transverse magnetization. The different routes that magnetization can follow through an experiment are known as *coherence transfer pathways*. In many multipulse experiments the magnetization may follow a number of coherence transfer pathways, even under ideal conditions. Magnetization following unwanted coherence pathways may distort measurements and, in the case multi-dimensional experiments, give rise to unwanted peaks or artifacts in the resulting spectrum.

Traditionally, magnetization that follows unwanted coherence transfer pathways arising from either source is eliminated by using *phase cycling*.¹⁹ Phase cycling is implemented by repeating an experiment several times using different phases (the axes about which the nuclear magnetization is rotated) for some or all of the pulses and then combining the resulting free induction decays in such a way that signals arising from unwanted pathways cancel out. For example, the inversion recovery pulse sequence for measuring longitudinal relaxation (T_1) consists of:

$$180^\circ, \tau, 90^\circ \text{ acquisition.} \quad (10)$$

The 180° pulse inverts the equilibrium magnetization which subsequently returns to equilibrium during τ due to T_1 relaxation. The extent of relaxation is monitored with the 90° pulse which converts the longitudinal magnetization into observable transverse magnetization. Any transverse magnetization arising due to the non-ideal behaviour of the 180° pulse will of course decay due to transverse relaxation during τ and this will introduce error into the measurement. Magnetization following this unwanted coherence transfer pathway can be eliminated by adding data acquired with equation 10 to that acquired with

$$180^\circ, \tau, 90^\circ \text{ acquisition.} \quad (11)$$

In this latter pulse sequence, the phase of the 180° pulse has been altered from x to $-x$. The result of this is that any transverse magnetization excited by the 180° pulse in the two cases will differ in phase by 180° and therefore undergo mutual cancellation when the free induction decays are coadded. In general, the more pulses there are in an experiment, the more phase cycling is necessary to eliminate unwanted coherence transfer pathways.

Phase cycling has a number of drawbacks, of which the most obvious is the additional time it takes to implement. Furthermore, phase cycling often works less than perfectly in practice, particularly when intense signals are to be removed; the reasons for this can include instrumental instability, sample spinning (if used), and an insufficient relaxation period for the magnetization to return to equilibrium between experiments. Dynamic range is also a frequent problem. The imperfections in phase cycling typically manifest themselves as artifacts in the spectrum or, in the case of two-dimensional experiments, as ridges of 't₁-noise' that may run right across the spectrum and can obscure peaks.

Magnetic field gradients offer the spectroscopist an alternative to phase cycling to remove unwanted magnetization. We have already noted that a magnetic field gradient can cause transverse magnetization to disappear completely, Figure 1b, and that this process can, if desired, subsequently be reversed by applying a refocusing pulse, Figure 2; both of these features can be exploited to allow phase cycling to be replaced with magnetic field gradient pulses in NMR experiments. For example, in the inversion recovery pulse sequence described above, the phase cycling can be replaced by a single magnetic field gradient pulse during τ to dephase any transverse magnetization excited by the 180° pulse. The gradient pulse must of course be applied for sufficient time to completely dephase the transverse magnetization; this time can be minimized by maximizing the strength of the gradient used. In this example, the use of gradient pulses

permits the experiment time to be halved, since only a single transient needs to be acquired with each τ value

In many experiments a radiofrequency pulse may bring about a number of coherence transfer processes of which only one is desired. For example, in experiments similar to that sketched in Figure 7, zero-, single- and double-quantum coherence may all be present during the evolution period t_1 and all may subsequently be detected following coherence transfer into observable single-quantum coherence, although only one process is of interest. A single process was traditionally isolated by using phase cycling. However, a single process can also be separated by exploiting the different sensitivities of different orders of coherence to magnetic field gradients and the fact that the pulse that brings about a coherence transfer process also acts as a refocusing pulse and gives rise to what is known as a *coherence transfer echo*.⁷ Coherence transfer echoes can be used to reverse the effects of magnetic field gradients in a similar way to spin echoes.²⁰ The main difference between a spin echo and a coherence transfer echo is that, with the latter, the coherence that is rephased after the refocusing/coherence transfer pulse is not the same as the one that was dephased before it. The formation of coherence transfer echoes after a 90° pulse is illustrated in Figure 13, where multiple to single-quantum coherence transfer processes are observed in the presence of a magnetic field gradient. The echoes arising from different coherence transfer processes occur at different times, reflecting the fact that while each multiple-quantum coherence dephases at a different rate, the observed single-quantum coherences all rephase at the same rate, regardless of their history. Clearly, if the gradient were switched off at the moment a particular coherence transfer echo is formed, only magnetization that has followed the corresponding coherence transfer pathway will be observed. In practice this is achieved by using magnetic field gradient pulses. For example, a single gradient pulse applied during t_1 will dephase all but the zero-quantum coherence and consequently only the zero to single-quantum coherence transfer process will be observed. Alternatively, if identical gradient pulses are applied during evolution and mixing and detection periods only the single-quantum to single-quantum process will be observed, analogously to the spin echo. To observe the double- to single-quantum coherence transfer process selectively it is necessary to apply a magnetic field gradient pulse during the detection period that is twice as long as that applied during the evolution period.

An example of a spectrum acquired using gradients to select a particular coherence transfer process is given in Figure 14.²¹

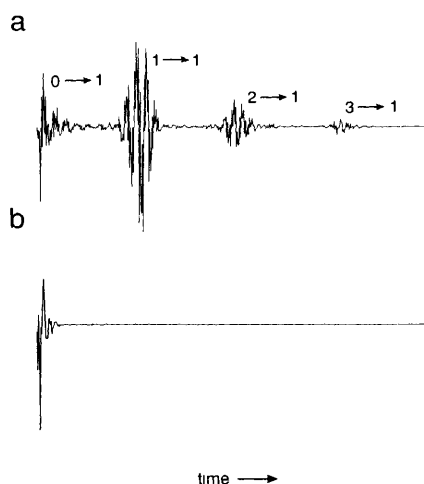


Figure 13 (a) Coherence transfer echoes forming in the presence of a magnetic field gradient after a dephasing period of 200 ms and a 90° coherence transfer pulse. The echoes arise from the transfer of zero-, single-, double-, and triple-quantum coherence to single-quantum coherence, as indicated, and occur at 0, 200, 400, and 600 ms respectively into the free induction decay. (b) Conventional free induction decay acquired under the same conditions for comparison.

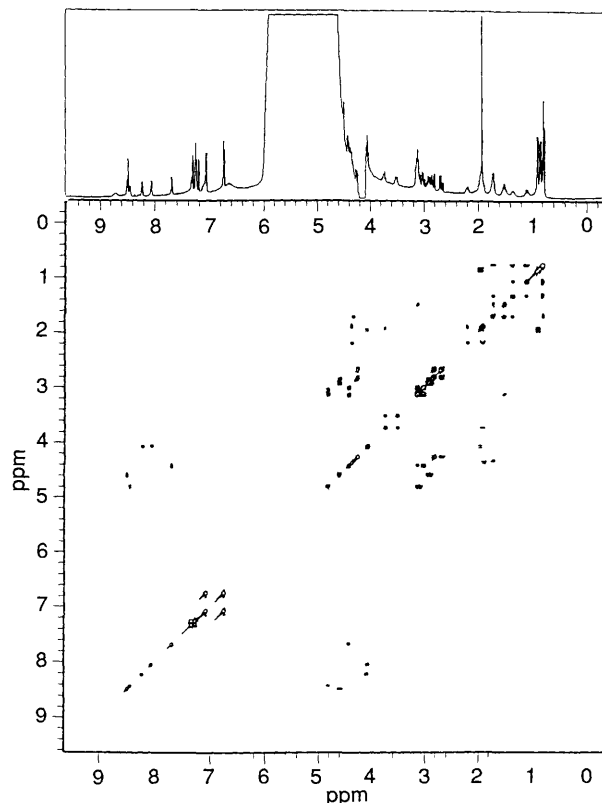


Figure 14 400 MHz ^1H double-quantum filtered COSY spectrum of 8 mM angiotensin II in H_2O . Coherence transfer pathway selection was achieved using magnetic field gradient pulses, no phase cycling was used.

(Reproduced, with permission, from ref 21, R Hurd, *J Magn Reson*, 1990, 87, 422)

Since this spectrum was acquired with a double-quantum filtered COSY experiment, only spins that can form double-quantum coherence (*i.e.* that are scalar coupled to at least one other spin) will be observed. Consequently the water peak, although dominating the conventional one-dimensional spectrum, is absent from the double-quantum filtered COSY spectrum except for a substantial ridge of t_1 -noise. The cleanliness with which the selection process has been achieved highlights a major advantage of using magnetic field gradient pulses: if the same experiment were attempted using phase cycling without using any other form of solvent suppression one would be unlikely to see anything but water in the resulting spectrum. The major disadvantage of using gradient pulses to select coherence transfer pathways is that up to 50% of the signal can be lost in some applications since in some contexts they can be more selective than phase cycling. Signal losses due to diffusion-attenuation can be minimized by keeping pairs of dephasing and rephasing gradient pulses close together and the amplitude of the gradient used to the minimum.

8 Conclusion

In the early days of NMR, magnetic field gradients were seen primarily as a problem, often hindering spectral analysis. However, over the past two and a half decades this perception has changed dramatically as the use of magnetic field gradients has made possible the measurement of diffusion, spawned magnetic resonance imaging, which is now a field in its own right, and most recently made possible the elimination of phase cycling in many experiments, allowing cleaner spectra to be obtained in shorter times. Even where unwanted magnetic field gradients remain a problem, particularly when large or heterogeneous samples are under study, techniques have been developed which have enabled many of the problems they pose to be overcome.

Acknowledgements. It is a pleasure to thank Drs. Suzanne Gilbert and Mark Horsfield for their many helpful comments while preparing this article, Dr. Steve Williams and the University of London NMR Imaging Facility at Queen Mary and Westfield College for Figure 11, and Professor Laurie Hall, Dr. Alan Fischer, and the Herchel Smith Laboratory for Medicinal Chemistry for Figure 12.

9 References

- 1 H. Y. Carr and E. M. Purcell, *Phys. Rev.*, 1954, **94**, 630.
- 2 R. Benn and H. Gunther, *Angew. Chem., Int. Ed. Engl.*, 1983, **22**, 350.
- 3 M. Gochin, D. P. Weitekamp, and A. Pines, *J. Magn. Reson.*, 1985, **63**, 431.
- 4 S. L. Duce, L. D. Hall, and T. J. Norwood, *J. Magn. Reson.*, 1990, **89**, 273.
- 5 S. Meiboom and D. Gill, *Rev. Sci. Instr.*, 1958, **29**, 688.
- 6 G. Bodenhausen, *Progr. NMR Spectrosc.*, 1981, **14**, 137.
- 7 R. R. Ernst, G. Bodenhausen, and A. Wokaun, 'Principles of Nuclear Magnetic Resonance in One and Two Dimensions', Clarendon Press, Oxford, 1987.
- 8 T. J. Norwood, *Progr. NMR Spectrosc.*, 1992, **24**, 295.
- 9 L. D. Hall and T. J. Norwood, *J. Chem. Soc., Chem. Commun.*, 1986, 44.
- 10 E. O. Stejskel and J. E. Tanner, *J. Chem. Phys.* 1965, **42**, 288.
- 11 P. Stilbs, *Progr. NMR Spectrosc.*, 1987, **19**, 1.
- 12 J. E. Tanner and E. O. Stejskel, *J. Chem. Phys.*, 1968, **49**, 1768.
- 13 T. J. Norwood, S. L. Duce, and L. D. Hall, *J. Magn. Reson. Series A*, 1993, **102**, 370.
- 14 D. Zax and A. Pines, *J. Chem. Phys.*, 1983, **78**, 6333.
- 15 P. B. Roemer, W. A. Edelstein, and J. S. Hickey, 'Book of Abstracts of the 5th Annual Meeting of the Society of Magnetic Resonance in Medicine', Montreal, August 19–22, 1986, p. 1067.
- 16 P. Lauterbur, *Nature*, 1973, **242**, 190.
- 17 M. A. Foster and J. M. S. Hutchison, *J. Biomed. Eng.*, 1985, **7**, 171.
- 18 B. J. Balcom, T. A. Carpenter, and L. D. Hall, *Can. J. Chem.*, 1992, **70**, 2693.
- 19 R. Freeman, 'A Handbook of Nuclear Magnetic Resonance', Longman Scientific & Technical, 1988.
- 20 A. Bax, P. G. De Jong, A. F. Mehlkopf, and J. Smidt, *Chem. Phys. Lett.*, 1980, **69**, 567.
- 21 R. E. Hurd, *J. Magn. Reson.*, 1990, **87**, 422.